27 February 1998

ELSEVIER

Chemical Physics Letters 284 (1998) 164–170

CHEMICAL PHYSICS LETTERS

Trapping-desorption and direct-inelastic scattering of HCl from MgO(100)

M. Korolik, D.W. Arnold [1], M.J. Johnson [2], M.M. Suchan, H. Reisler, C. Wittig

Department of Chemistry, University of Southern California, Los Angeles, CA 90089-0482, USA

Received 29 August 1997; in final form 21 November 1997

Abstract

A molecular beam of hyperthermal HCl ($J = 0$) impinges on a MgO(100) surface and the scattered HCl is probed state-selectively by using multiphoton ionization. Two regimes are identified. At incident energies of 0.54 and 0.90 eV, scattering is predominantly direct-inelastic, whereas at an incident energy of 0.11 eV, HCl is predominantly trapped and subsequently desorbs. For example, at 0.11 eV, the angular distribution of the HCl product is cosine-like, whereas at 0.54 and 0.90 eV, the scattered HCl is observed to peak near the specular angle. © 1998 Published by Elsevier Science B.V.

1. Introduction

Surfaces provide rich environments in which a variety of scientifically and technologically important chemical and physical processes take place. Consequently, much effort has gone into detailed examinations of the associated elementary processes. Prominent among these are molecule–surface interactions. Our understanding of such interactions has been advanced significantly by studies of molecule–surface collision dynamics, and both experimental and theoretical studies have been carried out for a number of systems, focusing primarily on metals [1–11]. Insulators have also been examined, but to a lesser extent [12–18].

An important change of scattering mechanism, i.e., from "trapping-desorption" to "direct-inelastic" scattering, takes place as the energy of the molecule–surface collision increases. Scattering that occurs via the trapping-desorption mechanism has been observed in systems with large molecule–surface binding energies and efficient translational energy loss channels (usually to surface phonons). For example, trapping-desorption in the NO/Pt(111) system occurs readily, presumably because of the large binding energy of 1.1–1.5 eV [3]. Alternatively, both trapping-desorption and direct-inelastic scattering have been observed in systems such as N_2/Cu(110) [8] and NO/graphite [12]. In addition, the intermediate "multiple scattering" regime has been identified, with extensive data recorded for the NO/graphite system [12].

Trapping into both dissociative chemisorption states and physisoption states with subsequent dissociation have been documented [19]. For the

[1] Present address: Sandia National Laboratory, Mail Stop 9671, Livermore, CA 94551-0969, USA.

[2] Present address: c/o Brian S. Orr, School of Chemistry, Macquarie University, Sydney NSW 2109, Australia.

PII S0009-2614(97)01421-8

HCl/MgO(100) system, we believe that trapping occurs only into a physisorption state.

In the present study, experimental data are presented which are interpreted as evidence for the transition from the trapping-desorption to the direct-inelastic scattering regimes in the HCl/MgO(100) system. The results are discussed in terms of the incident kinetic energy of the HCl molecule (E_{inc}), the angle of incidence (Θ_{inc}), surface corrugation, and the thermal energy associated with the surface temperature (T_s). Combining surface science and molecular beam techniques with quantum-state-selective laser detection enables the scattering dynamics of HCl from the MgO(100) surface to be examined in detail. Namely, quantum-state-selective detection allows us to investigate translational-to-rotational energy transfer, determine effects of surface vibrations on the rotational energy, and measure differential angular distribution of the scattered HCl. In addition, time-of-flight (TOF) measurements demonstrate the very long residence times of the trapped HCl.

2. Experimental

Pulsed HCl molecular beams were prepared by supersonic expansion of HCl diluted in suitable carriers. The beams impinged on a MgO(100) surface and the resulting state, angular, and TOF distributions of the scattered molecules were probed by using quantum-state-selective laser detection. Translational-to-rotational energy transfer was studied as a function of E_{inc}, Θ_{inc} and T_s.

E_{inc} was varied by changing the gas mixture. For example, seeding 1–2% HCl in 1.5–2.0 atm of Ne, He and H_2 at 300 K yields E_{inc} values of 0.11, 0.54 and 0.90 eV. Depending on the seeding conditions, from 75 to 90% of the HCl molecules were in the $J = 0$ rotational state, corresponding to rotational temperatures (T_{rot}) of 10–20 K.

The piezoelectric molecular beam nozzle (20 Hz, 150–250 μs pulse duration) directed the beam through a differentially pumped region and into the UHV chamber (base pressure $\sim 3 \times 10^{-10}$ Torr) which housed the MgO crystal. The surface to be studied was prepared by cleaving MgO along the (100) plane prior to mounting it on an XYZΘ manipulator and placing it in the UHV chamber. In order to remove contaminants and surface defects (oxygen deficiencies), the crystal was heated to 500°C for two hours in 10^{-5} Torr of oxygen. On a daily basis, Auger spectroscopy was used to check surface contamination, and surface order was verified by He diffraction.

HCl molecules were detected state-selectively by using (2 + 1) resonance enhanced multiphoton ionization (REMPI). To obtain the required radiation, the output of a dye laser was frequency doubled in BBO to generate tunable radiation near 238 nm having a linewidth of 0.7 cm^{-1} and an energy of approximately 0.75 mJ. The laser beam was focused into the UHV chamber with a 46 cm focal length lens. The REMPI signal (normalized by the square of the laser energy) provided a map of HCl rotational excitation. Rotational distributions were obtained at the specular angles for all of the Θ_{inc} values examined. When using the $V^1\Sigma^+ \leftarrow X^1\Sigma^+$ system and a 300 K ion cell (0.2–0.5 Torr), rotational line strengths for the ($v = 11$) ← ($v = 0$) band were found to be unity for $J = 0$–8, and were assumed to be unity for $J = 9$– 15 [11]. It was found that the Franck–Condon factor for the ($v = 12$) ← ($v = 0$) band (used to detect $J = 9$–12) is smaller than that for ($v = 11$) ← ($v = 0$) by the factor 1.55 ± 0.10. Likewise, the Franck–Condon factor for the ($v = 13$) ← ($v = 0$) band (used to detect $J = 13$–15) is smaller than that for ($v = 11$) ← ($v = 0$) by the factor 2.35 ± 0.10.

Angular distributions of scattered molecules were obtained by moving the probe laser along an arc centered at the molecular beam- surface collision point and collecting signal at the Q(4) line of the $E^1\Sigma^+(v = 0) \leftarrow X^1\Sigma^+(v = 0)$ transition. A different laser system (0.12 cm^{-1} linewidth at 238 nm, ~ 2.5 mJ) was used to acquire angular distributions at $E_{inc} = 0.11$ eV.

Temporal profiles of scattered molecules were obtained by recording signal at the $E^1\Sigma^+(v = 0) \leftarrow X^1\Sigma^+(v = 0)$ Q(2) transition as a function of the delay between the probe laser and nozzle triggers.

Though the present application of the REMPI technique measured number density rather than flux, a flux-to-density transformation was not applied to the rotational state distributions, since the scattered HCl velocity distributions are unknown. We estimate

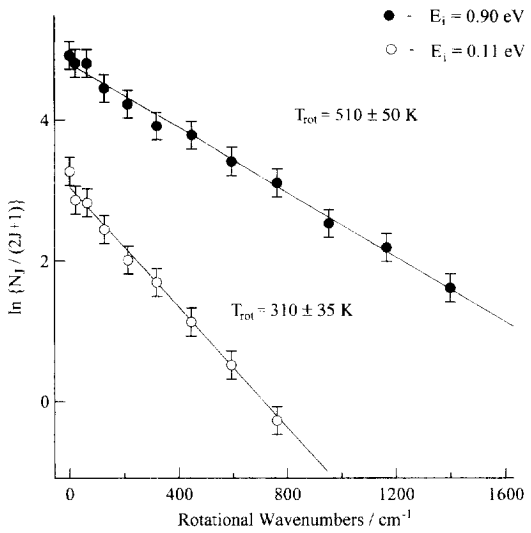

Fig. 1. Boltzmann plots for HCl scattered from 300 K MgO(100) at E_{inc} values of 0.11 and 0.9 eV (Θ_{inc} = 15°). The lines are least squares fits.

that such corrections are smaller than the error bars of the measurements.

3. Results

Scattered HCl ($v = 0$) rotational state and angular distributions were recorded while varying collisional conditions such as E_{inc}, Θ_{inc} and T_s. Data were collected for E_{inc} values of 0.11, 0.54 and 0.90 eV. The production of HCl ($v = 1$) was below the detection sensitivity (i.e., $< 1\%$ at $E_{inc} = 0.90$ eV and $\Theta_{inc} = 0°$).

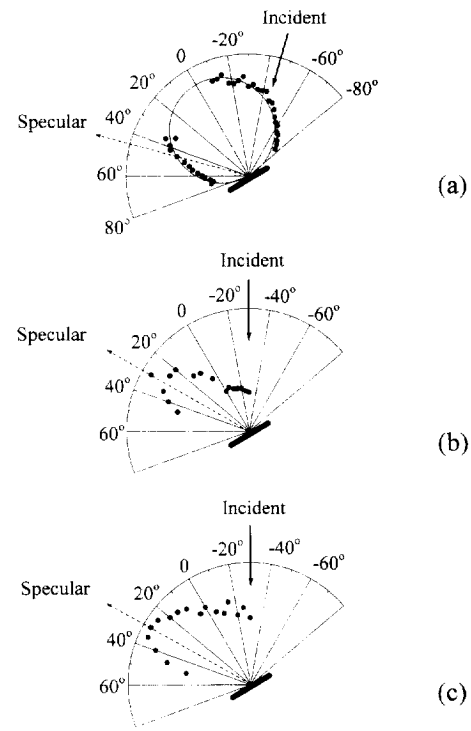

Fig. 3. Angular distributions for HCl ($J = 4$) scattered from 300 K MgO(100) at: (a) $E_{inc} = 0.11$ eV and $\Theta_{inc} = 45°$; (b) $E_{inc} = 0.54$ eV and $\Theta_{inc} = 30°$; (c) $E_{inc} = 0.90$ eV and $\Theta_{inc} = 30°$. Data were not recorded in the range $-10° \leq \Theta_{inc} \leq 30°$ due to an obstruction. The solid line is a cosine function.

Two scattered HCl rotational distributions are

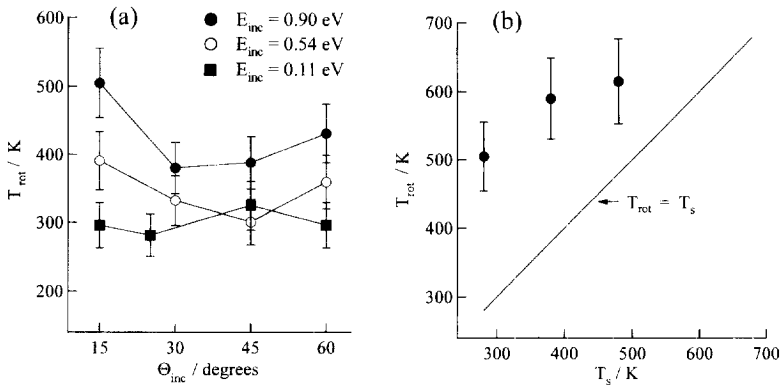

Fig. 2. (a) T_{rot} values of scattered HCl versus Θ_{inc} at $E_{inc} = 0.11$, 0.54 and 0.90 eV (T_s = 300 K); (b) T_{rot} values of scattered HCl versus T_s at $E_{inc} = 0.90$ eV and $\Theta_{inc} = 15°$.

shown in Fig. 1. The good degree of linearity displayed in Fig. 1 was observed for all such plots, enabling the rotational distributions to be characterized by a parameter, T_{rot}. In general, T_{rot} values increased with E_{inc} (Fig. 2a). For example, for E_{inc} values of 0.54 and 0.90 eV, T_{rot} was 390 and 510 K, respectively, for $T_s = 300$ K and $\Theta_{inc} = 15°$. However, a qualitative difference was observed for $E_{inc} = 0.11$ eV, where T_{rot} was found to be 310 ± 35 K for $T_s = 300$ K and all values of Θ_{inc}. In this case, the observation that $T_{rot} \approx T_s$ suggests that the HCl molecules may have resided on the surface long enough to equilibrate their rotational degree of freedom with the surface.

Surface temperature effects on T_{rot} were determined at $E_{inc} = 0.90$ eV and $\Theta_i = 15°$. When T_s was increased from 280 to 480 K, T_{rot} increased from 505 to 615 K (Fig. 2b). At $E_{inc} = 0.90$ eV, T_{rot} always exceeded T_s.

Angular distributions for scattered HCl ($v = 0$, $J = 4$) are shown in Fig. 3. Again, there is a qualitative difference between $E_{inc} = 0.11$ eV and the higher E_{inc} values of 0.54 and 0.90 eV. For 0.11 eV (Fig. 3a), HCl leaves the surface with a cosine-like distribution (solid line). In contrast, scattering at the higher energies yields distributions which are peaked near the specular direction. Note that the near-specular lobe obtained at $E_{inc} = 0.90$ eV (Fig. 3c) is broader than the one obtained at $E_{inc} = 0.54$ eV (Fig. 3b).

Temporal profiles of scattered HCl ($v = 0$, $J = 2$) were recorded at $E_{inc} = 0.11$ eV for T_s values from 150 to 188 K, as shown in Fig. 4. They are compared to the HCl ($v = 0$, $J = 0$) incident pulse. It is clear that for $T_s < 188$ K the scattered temporal profiles have tails that extend to long times. For $T_s = 150$ K, the tail can be fitted by an exponential having a time constant of 1.2 ms. Both the incident and scattered profiles were obtained at the same probe position with a probe-surface distance $\leq$ 1 mm. Though the scattered HCl is delayed because of its flight time, this accounts for only a few microseconds, which is insignificant on the time scale of Fig. 4.

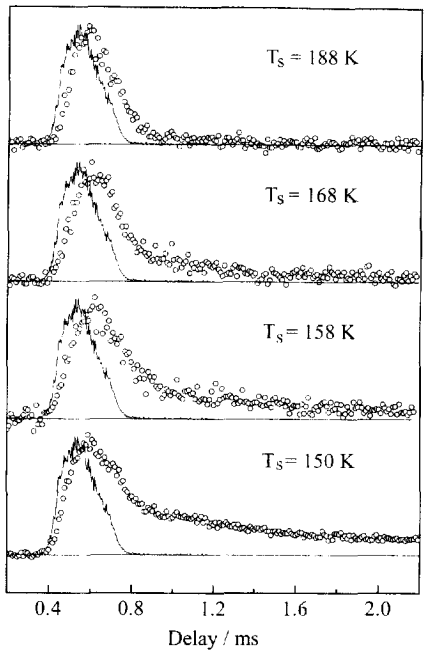

Fig. 4. Temporal profiles of incident HCl ($J = 0$) (solid line) and scattered HCl ($J = 2$) (open circles) at $E_{inc} = 0.11$ eV and $\Theta_{inc} = 15°$ for different values of T_s. The incident beam profile was recorded without the surface present.

4. Discussion

The experimental results reported herein are consistent with a molecule–surface scattering mechanism that changes from predominantly trapping-desorption at $E_{inc} = 0.11$ eV to predominantly direct-inelastic at $E_{inc} = 0.54$ and 0.90 eV. This is the main conclusion of the present work. As discussed below, the evidence in support of this includes angular and product state distributions of the scattered HCl, as well as the time-resolved scattering studies carried out at 0.11 eV with different surface temperatures. Since no PES is available for the HCl/MgO(100) system, it is not possible to carry out a detailed comparison between theory and experiment. Thus, our present level of understanding is qualitative.

Similar observations of the transition between the trapping-desorption and the direct-inelastic scattering regimes have been reported by Sitz and coworkers for N_2 scattered from Cu(110) [8] and Si(100) [20], and by Walther and coworkers, who have carefully examined the NO/graphite system [12]. A complementary study of HCl undergoing direct-inelastic scattering from Au(111) has been reported by Lykke and Kay [11].

4.1. Trapping-desorption

The binding energy and geometry of physisorbed HCl on MgO(100) are of considerable importance for the problem at hand. Though these properties have not been determined experimentally, McCarthy et al. [21] have carried out electronic structure calculations on this system, including a correction for the electrostatic interaction of the HCl dipole with the ionic surface. They find well depths of 0.35 and 0.50 eV, respectively (the latter being the global minimum), for the cases of the HCl dipole parallel to the surface and perpendicular to the surface with the hydrogen facing the oxygen anion. This illustrates the large anisotropy of the potential, which suggests that steering may play an important role in the dynamics [22].

The trapping of incident HCl is the result of energy transfer from HCl translational motion to the crystal phonons. As the vibrationally and rotationally cold HCl molecules approach the surface, they are accelerated and steered in the attractive, anisotropic potential. Because the surface is highly polar and corrugated, the parallel component of the linear momentum of the incident HCl may not be conserved, in contrast to most metal surfaces [11]. Rebounding HCl molecules can be trapped if their normal kinetic energy is less than the molecule–surface binding energy. In this case, the molecules do not escape directly, but are either trapped right away or return to the surface where further scattering occurs. These complex scattering processes can lead to results which are intermediate between direct inelastic and trapping-desorption, e.g., scattering that is not localized around the specular lobe (relative to direct-inelastic) but does not display full surface accommodation.

Desorption of molecules which have been trapped occurs when the molecule–surface coordinate accumulates energy in excess of the well depth (for the case of no exit barrier). This results in rotational and translational distributions that are close to equilibrium distributions at the surface temperature. Note that a cosine-like angular distribution of desorbing molecules is expected on the basis of arguments similar to those used to describe effusion from a pinhole [23]. For a pre-exponential factor of $10^{13\pm1}$ Hz in the Arrhenius equation [24], binding energies in the range 0.35–0.50 eV yield residence times in the range 10 ns–100 μs for $T_s = 300$ K. Thus, molecules that undergo trapping have mean residence times on the surface that are very long relative to the time scale of molecule–surface vibrations.

The present experimental results are consistent with a mechanism in which the majority of the low-E_{inc} incident molecules (i.e., 0.11 eV) become trapped during the molecule–surface collision. Thus, these molecules become equilibrated at the surface temperature and re-enter the gas phase via desorption, which occurs long after the initial encounter. For example, note the angular dependence shown in Fig. 3a, which shows the cosine-like angular distribution of the scattered HCl. This angular distribution differs qualitatively from those at the higher E_{inc} values, the latter showing preference for scattering near the specular angle. Likewise, the T_{rot} values shown in Fig. 2a show that the HCl rotational excitation is Boltzmann-like at approximately T_s. This differs from the rotational distributions obtained at the higher E_{inc} values, in which T_{rot} is higher than T_s.

The time-resolved desorption results shown in Fig. 4 illustrate the long residence times. Clearly, there is more than a single desorption rate, and the kinetics that give rise to such data may be complex. From the slow-decay component (using $k = \nu \exp\{-\Delta H/kT\}$, with $\nu = 10^{13}$ s^{-1}), a ΔH value of ~ 0.3 eV is inferred, which is somewhat lower than the estimate of McCarthy et al. [21].

Thus, all of the experimental data taken at 0.11 eV are in agreement with the predominance of a trapping-desorption mechanism.

4.2. Direct-inelastic scattering

As mentioned above, the results obtained in the present experiments at the higher E_{inc} values differ qualitatively from those obtained at $E_{inc} = 0.11$ eV. Namely, at 0.54 and 0.90 eV, the scattered HCl molecules are found to lie preferentially in lobes near the specular angle, which is consistent with the predominance of a direct-inelastic scattering mechanism. From the angular distributions shown in Fig. 3, it appears that there may be some trapping and/or multiple scattering at these higher E_{inc}, but the dominance of the near-specular lobe is clear. In addition,

for the near-specular lobe, the rotational and translational degrees of freedom are not equilibrated with the surface (Fig. 2a), again in agreement with a direct-inelastic scattering mechanism.

Angular distributions have proven to be useful tools for unraveling the dynamics of molecule–surface scattering. In the present study, the angular distribution were seen to broaden when E_{inc} was changed from 0.54 to 0.90 eV. In most of the systems studied to date, the angular distributions of scattered molecules have been observed to *narrow* at higher collision energies, due to the fact that, as the collision energy is increased, the surface thermal energy becomes progressively less important [11,18]. However, broadening of the angular distribution at higher energies has been observed in $N_2/W(100)$ [25], $O_2/Ag(111)$ [26] and Xe/Pt(111) [27]. We tentatively attribute the broadening observed in the present study to an increase of the effective MgO(100) corrugation at the higher collision energies. The MgO(100) corrugation (i.e., 0.32–0.46 Å, as determined from He scattering at 25–150 meV [28–30]), is smaller than the 0.68 Å expected by interpreting the ionic radii of the Mg^{+2} and O^{-2} ions. At least part of this difference may be attributed to surface charge redistribution, which provides a modest amount of covalent bonding [31,32]. It is known that corrugation broadens angular distributions relative to flat surfaces [10], and at the higher incident energies, HCl recoils from turning points which are closer to the surface nuclei, thus experiencing larger corrugation.

An additional mechanism for broadening of the specular lobe arises from the fact that at higher incident energies the translational energy losses increase [7]. Scattered molecules that lose more parallel than normal momentum scatter in a subspecular direction, whereas those that lose more normal than parallel momentum scatter in a supraspecular direction. In other words, dispersion in the parallel and normal components of the momentum can contribute to angular broadening. In the present case, HCl translational energy losses become larger at the higher incident energies, and this can broaden the specular lobe.

Comparing the results obtained by using HCl/MgO(100) to those obtained by using HCl/Au(111) [11] can provide insight into differences in the scattering of polar molecules from insulator versus (rather inert) metal surfaces. The main differences that have been observed are the participation of a trapping-desorption channel at low E_{inc} for the HCl/MgO(100) system, as well as the higher efficiency of $kT_s \rightarrow E_{rot}$ energy transfer (0.55 ± 0.2) at high E_{inc} compared to the HCl/Au(111) system, where the energy transfer efficiency is 0.08 [11]. Also, as mentioned above, the angular distributions of HCl scattered from Au(111) become narrower as E_{inc} increases, which is opposite to the dependence observed in HCl/MgO(100). In addition, normal energy scaling is observed in HCl/Au(111) but not in HCl/MgO(100).

All of the above differences between the two systems can be rationalized as due to a larger attractive well for HCl/MgO(100) compared to HCl/Au(111) (which is believed to be approximately 0.23 eV [11]) as well as larger corrugation for MgO(100) than Au(111). Note that corrugation may also enhance $kT_s \rightarrow E_{rot}$ energy transfer.

In summary, we conclude that the present data reflect the transition from trapping-desorption to direct inelastic scattering, as has been observed previously [8,12], in fact even in one of the earliest studies of molecule–surface scattering [33]. The present results have a great deal in common with the studies of Walther and coworkers on NO/graphite [12]. Likewise, similar observations of this change of scattering mechanism have been reported by Sitz and coworkers for N_2 scattering from Cu(110) [8] and Si(100) [19].

Acknowledgements

This research was supported by the U.S. Air Force Office of Scientific Research. The authors benefited from discussions with G. Sitz, B. Kay and B. Koel. The reviewer's comments were especially helpful.

References

[1] G.D. Kubiak, J.E. Hurst Jr., H.G. Rennagel, G.M. McClelland, R.N. Zare, J. Chem. Phys. 79 (1983) 5163.
[2] R.J. Hamers, P.L. Houston, R.P. Merrill, J. Chem. Phys. 88 (1988) 6548.

[3] W.L. Guthrie, T.-H. Lin, S.T. Ceyer, G.A. Somorjai, J. Chem. Phys. 76 (1982) 6398.
[4] D.C. Jacobs, K.W. Kolasinski, S.F. Shane, R.N. Zare, J. Chem. Phys. 91 (1989) 3182.
[5] G.O. Sitz, A.C. Kummel, R.N. Zare, J. Chem. Phys. 89 (1988) 2558.
[6] T.F. Hanisco, A.C. Kummel, J. Chem. Phys. 99 (1993) 7076.
[7] M.E.M. Spruit, P.J. van den Hoek, E.W. Kuipers, F.H. Geuzebroek, A.W. Kleyn, Surf. Sci. 214 (1989) 591.
[8] J.L.W. Siders, G.O. Sitz, J. Chem. Phys. 101 (1994) 6264.
[9] J.L.W. Siders, G.O. Sitz, J. Vac. Sci. Technol. A 13 (1995) 1400.
[10] J. Misewich, M.M.T. Loy, J. Chem. Phys. 84 (1986) 1939.
[11] K.R. Lykke, B.D. Kay, J. Chem. Phys. 92 (1990) 2614.
[12] D. Glatzer, J. Häger, M. Fink, H. Walther, Surf. Sci. 374 (1997) 169; J. Häger, D. Glatzer, H. Kuze, M. Fink, H. Walther, Surf. Sci. 374 (1997) 180.
[13] D. Ettinger, K. Honma, M. Keil, J.C. Polanyi, Chem. Phys. Lett. 87 (1982) 413.
[14] J.W. Hepburn, F.J. Northrup, G.L. Ogram, J.C. Polanyi, J.M. Williamson, Chem. Phys. Lett. 85 (1982) 127.
[15] E. Kolodney, D. Baugh, P.S. Powers, H. Reisler, C. Wittig, Chem. Phys. Lett. 145 (1988) 177.
[16] E. Kolodney, A. Amirav, R. Elber, R.B. Gerber, Chem. Phys. Lett. 111 (1984) 366.
[17] C. Roth, J. Häger, H. Walther, J. Chem. Phys. 97 (1992) 6880.
[18] T.W. Francisco, N. Camillone, R.E. Miller, Phys. Rev. Lett. 77 (1996) 1402.
[19] S. Ceyer, Ann. Rev. Phys. Chem. 39 (1988) 479.
[20] J.L.W. Siders, G.O. Sitz, SPIE Proc. (1995) 2547.
[21] M.R. Chacontaylor, M.I. McCarthy, J. Phys. Chem. 100 (1996) 7610.
[22] M. Kay, G.R. Darling, S. Holloway, J.A. White, D.M. Bird, Chem. Phys. Lett. 245 (1995) 311.
[23] M. Knudsen, Ann. Phys. 48 (1915) 1113.
[24] A. Zangwill, Physics at Surfaces, Cambridge University Press, Cambridge, 1988, p. 362.
[25] C.T. Rettner, Surf. Sci. 204 (1988) L677.
[26] M.E.M. Spruit, P.J. van den Hoek, E.W. Kuipers, F.H. Geuzebroek, A.W. Kleyn, Phys. Rev. B 39 (1989) 3915.
[27] C.T. Rettner, J.A. Barker, D.S. Bethune, Phys. Rev. Lett. 67 (1991) 2183.
[28] K.H. Rieder, Surf. Sci. 118 (1982) 57.
[29] G. Brusdeylins, R.B. Doak, J.G. Skofronick, J.P. Toennies, Surf. Sci. 12 (1983) 191.
[30] E. Kolodney, A. Amirav, Surf. Sci. 155 (1985) 715.
[31] M. Sidoumou, V. Panella, J. Suzanne, J. Chem. Phys. 101 (1994) 6338.
[32] U. Birkenheuer, J.C. Boettger, N. Rosch, J. Chem. Phys. 100 (1994) 6826.
[33] J.E. Hurst, C.A. Becker, J.P. Cowin, K.C. Janda, L. Wharton, D.J. Auerbach, Phys. Rev. Lett. 43 (1979) 1175.